Gynecologic Oncology 162 (2021) 517–525

Contents lists available at ScienceDirect

Gynecologic Oncology

journal homepage: www.elsevier.com/locate/ygyno

Review Article

# The feasibility of folate receptor alpha- and HER2-targeted intraoperative fluorescence-guided cytoreductive surgery in women with epithelial ovarian cancer: A systematic review

J.M. de Jong [a], J.P. Hoogendam [a], A.J.A.T. Braat [b], R.P. Zweemer [a], C.G. Gerestein [a,*]

[a] Department of Gynaecological Oncology, University Medical Center Utrecht, Utrecht, the Netherlands
[b] Department of Nuclear Medicine, University Medical Center Utrecht, Utrecht, the Netherlands

## HIGHLIGHTS

- Targeted fluorescence-guided cytoreductive surgery is feasible in women with epithelial ovarian cancer positive for FRα.
- True positive and false positive values ranged from 75 to 77% and 10–25%, respectively.
- FRβ-expressing macrophages in lymph nodes cause a cross-reaction with the FRα-targeted imaging agents.

## ARTICLE INFO

*Article history:*
Received 4 March 2021
Accepted 20 May 2021
Available online 28 May 2021

## ABSTRACT

*Background.* Epithelial ovarian cancer (EOC) is often diagnosed late, with a 5-year relative survival of 30.2% for patients with metastatic disease. Residual disease following cytoreductive surgery is an important predictor for poor survival. EOC is characterized by diffuse peritoneal metastases and depositions of small size, challenging a complete resection. Targeted fluorescence imaging is a technique to enhance tumor visualization and can be performed intraoperatively. Folate receptor alpha (FRα) and human epidermal growth factor receptor 2 (HER2) are overexpressed in EOC in 80% and 20% of the cases, respectively, and have been previously studied as a target for intraoperative imaging.

*Objective.* To systematically review the literature on the feasibility of FRα and HER2 targeted fluorescence-guided cytoreductive surgery (FGCS) in women with EOC.

*Methods.* PubMed and Embase were searched for human and animal studies on FGCS targeting either HER2 or FRα in either women with EOC or animal models of EOC. Risk of bias and methodological quality were assessed with the SYRCLE and MINORS tool, respectively.

*Results.* All animal studies targeting either FRα or HER2 were able to detect tumor deposits using intraoperative fluorescence imaging. One animal study targeting HER2 compared conventional cytoreductive surgery (CCS) to FGCS and concluded that FGCS, either without or following CCS, resulted in statistically significant less residual disease compared to CCS alone. Human studies on FGCS showed an increased detection rate of tumor deposits. True positives ranged between 75%–77% and false positives between 10%–25%. Lymph nodes were the main source of false positive results. Sensitivity was 85.9%, though only reported by one human study.

*Conclusion.* FGCS targeting either HER2 or FRα appears to be feasible in both EOC animal models and patients with EOC. FGCS is a promising technique, but further research is warranted to validate these results and particularly study the survival benefit.



**Contents**



* Corresponding author at: Department of Gynaecological Oncology, Division Cancer Center, University Medical Centre Utrecht, F05.126, PO Box 85500, Utrecht 3508 GA, the Netherlands.
*E-mail address:* c.g.gerestein-2@umcutrecht.nl (C.G. Gerestein).

https://doi.org/10.1016/j.ygyno.2021.05.017

## 1. Introduction

In the United States, every year 21,750 women are diagnosed with ovarian cancer, of which >90% is of epithelial origin. Symptoms of ovarian cancer are vague and often present late, causing 75% of the patients to be diagnosed at an advanced stage [1]. Current 5-year relative survival for women with epithelial ovarian cancer (EOC) is 48.6% according to the SEER program of the U.S. National Cancer Institute, ranging from 30.2% at a distant stage and 92.6% at a localized stage. Standard treatment of advanced stage EOC is cytoreductive surgery and platinum-based chemotherapy. The goal of cytoreductive surgery is a complete resection of all visible tumor tissue, considering postoperative residual disease is an important predictor of survival [2–6]. Tumor lesions are detected by preoperative CT-scans and visual inspection and palpation during surgery. The identification of small tumor deposits can be challenging. A personalized intraoperative tumor detection strategy could facilitate the surgeon in achieving complete cytoreduction and possibly increase survival.

With fluorescence imaging, tumor cells are made visible by a fluorescent probe conjugated to a specific tumor targeting molecule. These imaging agents can be designed for different types of cancers with different molecular characteristics [7]. The goal of implementing this technique intraoperatively is to improve detection of peritoneal micrometastases, defined as tumor deposits that are between 0.2 mm and 2.0 mm in diameter, and to increase complete resection rate.

Promising targets to implement in this technique are folate receptor alpha (FRα) and human epidermal growth factor receptor 2 (HER2). FRα is one of the three isoforms of the folate receptor. It binds folate, which is essential for DNA replication during mitosis and meiosis. FRα is overexpressed in approximately 80% of the EOCs, making it an interesting target for fluorescence-guided cytoreductive surgery (FGCS) [8–10]. FRα is overexpressed in various cancer types besides EOC and has been previously studied as a target for intraoperative imaging in lung cancer [11–13]. HER2, a transmembrane protein tyrosine kinase receptor, is overexpressed in approximately 20% of EOCs [14–16]. Heterodimerization of HER2 with other receptors of the EGFR-family, occurring more frequently in case of HER2 overexpression, induces cell proliferation, cell migration and resistance to apoptosis [17]. HER2 is used as a therapeutic target in HER2-positive breast cancer and gastric cancer, although it may be applicable to other cancer types as well, including EOC [18,19]. As a target used in intraoperative imaging, HER2 has been studied in animal models of, among others, lung cancer and breast cancer [20,21].

Since FRα and HER2 are overexpressed in EOC and have been previously successfully studied as targets for intraoperative imaging in other cancer types, they are considered to be suitable targets for FGCS in the treatment of EOC as well. The objective of this review is to critically assess the feasibility of FRα- and HER2-targeted FGCS in women with EOC.

## 2. Methods

### 2.1. Search strategy and eligibility criteria

This review was written in adherence to the PRISMA guidelines. PubMed and Embase were searched on June 18, 2020. The search string included terms on FGCS, epithelial ovarian cancer and the targets of interest (supplementary files S1 and S2). We included studies on FGCS targeting either HER2 or FRα in either women with EOC or animal models of EOC and were written in English.

### 2.2. Study selection

Duplicates of selected studies were removed. Studies were screened for title and abstract by one researcher (JJ) to select eligible studies. Full texts were obtained and assessed for their eligibility by one researcher (JJ). When uncertain if a study met the inclusion criteria, the study was discussed with a second researcher (CG) to achieve consensus.

### 2.3. Data extraction

The following data, if available, were extracted from the original articles: true positive, false positive, false negative and true negative resected lesions, number of resections, sensitivity, positive predictive value, tumor-to-reference ratio of false and true positive resected lesions, duration of in vivo imaging, visual detection of tumor deposits

versus fluorescence-guided detection of tumor deposits, pharmacokinetics, and adverse events. FGCS and fluorescence-guided detection of tumor deposits were determined as successful if fluorescent peritoneal tumor deposits could be detected. In all studies, resected deposits were histologically examined to determine tumor status. Tumor-to-reference ratio indicates the uptake of a fluorescent imaging agent, normalized to a reference signal such as muscle or background.

### 2.4. Quality of evidence

Assessment of risk of bias and methodological quality was performed for all included studies. Human studies were assessed for methodological quality using the MINORS (Methodological Index for Non-Randomized Studies) tool [22]. This tool was developed specifically for non-randomized studies, either comparative or non-comparative.

Animal studies were assessed for risk of bias using the SYRCLE (Systematic Review Center for Laboratory animal Experiments) tool [23]. This tool is based on the Cochrane risk of bias tool [24] and has been adapted to assess the risk of bias in animal-based research.

## 3. Results

### 3.1. Study selection

A total of 219 studies were exported, 102 from PubMed and 117 from Embase (Fig. 1). 42 duplicates were identified and removed. Screening of title and abstract resulted in exclusion of 157 studies, with 20 articles remaining. Full text could be obtained for all studies. Screening of full text identified 13 eligible articles. Reasons for exclusion were wrong outcome measure (five studies), incorrect intervention (one study) and wrong publication type (one study). No human studies and five animal studies were included for HER2. Six human studies and three animal studies were included for FRα.

The substantial methodological and statistical heterogeneity precluded a meta-analysis on the retrieved studies.

### 3.2. Risk of bias

#### 3.2.1. Animal studies

Risk of bias assessment for animal studies is summarized in supplementary fig. S3. Bias in sequence generation, allocation concealment, random housing and incomplete outcome data was unclear for all studies. No study except Debie et al. (2018) reported on differences in baseline characteristics [25]. Bias in blinding of caregivers/investigators, random outcome assessment and blinding of outcome assessor was not applicable to all studies, since they investigated only one tumor model and one intervention or were non-comparative studies. Risk of reporting bias was detected in two studies, where the number of animals reported in the methods did not correspond to the results or was unclear overall [26,27]. Debie et al. (2018) reported two authors who are co-inventors of a patent related to the imaging agent [25]. Hekman et al. (2017) reported two authors with competing financial interest due to relations with the company providing part of the imaging agent [28].

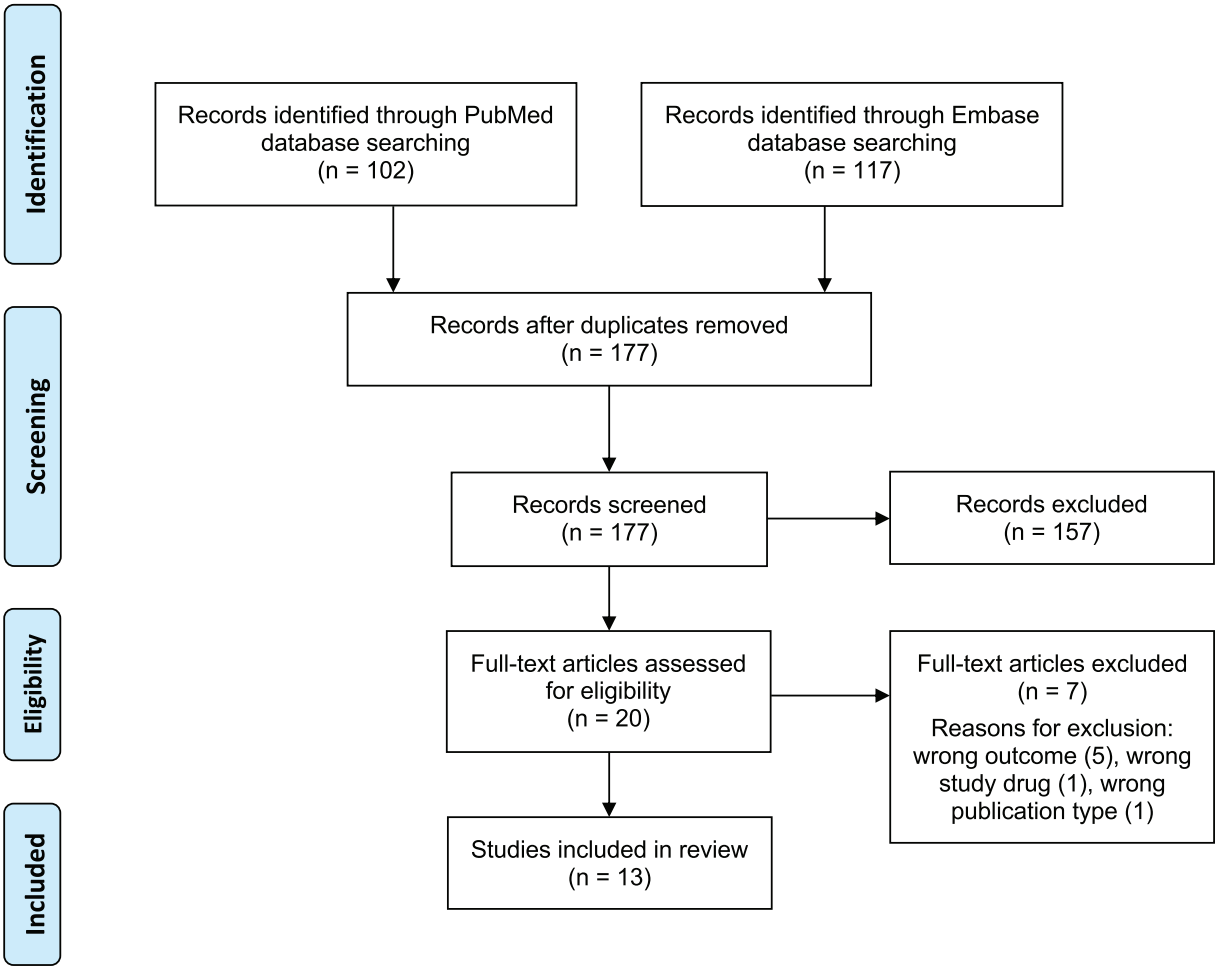


**Fig. 1.** Flow diagram of the inclusion process.

*3.2.2. Human studies*

Methodological quality assessment for human studies is summarized in supplementary fig. S4. Overall methodological quality was good. Blinding of the outcome assessor was reported and adequate in all studies, except for one unblinded study [29]. Prospective study size calculation was not reported in three out of six studies.

*3.3. HER2 - Animal studies*

*3.3.1. Population characteristics*

Population characteristics are summarized in Table 1. All studies were performed in immunodeficient female mice. Age of the mice was reported by three studies. As a model for EOC, SKOV3 cells, either Luciferin transfected or not, were used by all studies. Four studies injected tumor cells intraperitoneally, one study injected tumor cells orthotopically. Imaging systems used were either Fluobeam, Maestro, FluorVivo or a prototype camera system. Imaging agents consisted of a fluorescent component coupled to a targeting component. As a fluorescent component, IRDye800CW was used in three studies. The two other studies used either Alexa680 or Rhodamine Green as the fluorescent component. Most common targeting component was the antibody trastuzumab (three out of of five studies), while the other studies used either pertuzumab or an anti-HER2 nanobody.

## 4. Results

Fluorescence-guided detection of HER2 positive tumor deposits was successful for all studies [25,27,30–32]. Results are summarized in Table 2. Smallest nodules detected using intraoperative fluorescence imaging ranged from 0.5 to 1 mm [30,31]. One study that used luciferin-transfected SKOV3 cells for tumor inoculation measured tumor load with bioluminescence imaging before and after surgical intervention, enabling the researchers to quantify the effect of different surgical interventions on residual disease [25]. After conventional cytoreductive surgery (CCS), 19.6% of resections were false positives and the sensitivity was 59.3%. After CCS, researchers performed FGCS to study the added effect of this surgical intervention on residual disease. False positives increased with 6.1% to 25.7%, however sensitivity increased to 95.4%. Residual disease, of any size, showed a decrease from 2.9% to 0.7% ($p < 0.05$). When performing FGCS alone, sensitivity was 99.0% and residual disease was 1.1%. From these results, the authors concluded that FGCS, either without or following CCS, performed better than CCS alone to reduce residual disease.

Longmire et al. (2009) used spectral fluorescence imaging as a reference standard for the detection of fluorescent signal [32]. Results of spectral fluorescence imaging and real-time fluorescence imaging were comparable with a true positive of 52.3%, a false positive of 2.3%, a true negative of 43% and a false negative of 2.3%.

The tumor-to-reference ratio was reported by two studies. One study reported a mean tumor-to-muscle ratio of 22.2, another study reported a mean tumor-to-background ratio (TBR) of 14.4 [25,27].

*4.1. FRα – Animal studies*

*4.1.1. Population characteristics*

Population characteristics are summarized in Table 3. All studies were performed in immunodeficient mice. Sex and age of the mice were reported by one and two studies, respectively. Two studies used IGROV1 cells for tumor inoculation. One study used isolated primary cells from tumor samples taken from patients with serous ovarian cancer. All studies injected tumor cells intraperitoneally. The imaging system used was reported by two studies and was either the IVIS Lumina or the FloCam interchanged with a prototype camera system. The imaging agents used by the included studies contained porphyrin, IRDye800CW or FITC as the fluorescent component. The targeting component was either farletuzumab or folate.

**Table 1**
Population characteristics for animal studies studying HER2-targeted FGCS. Abbreviations: i.p. (intraperitoneally), i.v. (intravenously), TMR (tumor-to-muscle ratio), TBR (tumor-to-background ratio), TP (true positive), FP (false positive), TN (true negative), FN (false negative).

| Author, year | Sex | Age | Type | N | Tumor model | Imaging system | Imaging agent | Outcome |
|---|---|---|---|---|---|---|---|---|
| Lee [27] | Female | 6–8 weeks | Nude mice | 5 | $1 \times 10^6$ SKOV3, orthotopically | Fluobeam (Fluoptics) | 89Zr-Df-pertuzumab-IRDye800CW, i.v. | TMR |
| Debie [25] | Female | | Crl:NU-Foxn1$^{nu}$ mice | 13 | $0.5 \times 10^6$ SKOV3$^{fluc+}$, i.p. | Fluobeam (Fluoptics) | 2 nmol 2Rs15dCys-IRDye800CW, i.v. | Number of nodules detected, TP, FP, TN, FN, TBR, surgery duration, residual tumor |
| Terwisscha [30] | Female | 6–8 weeks | BALB/c nude mice | 5 | $5 \times 10^6$ SKOV3$^{luc+}$, i.p. | Prototype camera system | 100 μg trastuzumab-IRDye800CW, i.p. | Smallest nodule size |
| Kosaka [31] | Female | 6–8 weeks | Nude mice | 4 | $2 \times 10^6$ SKOV3, i.p. | Maestro (Caliper LifeSciences) | 50 μg trastuzumab-Alexa680, i.p. | Number of nodules detected, TP, smallest nodule size |
| Longmire [32] | Female | | Nude mice | 5 | $2 \times 10^6$ SKOV3, i.p. | FluorVivo (INDEC Biosystems) | Trastuzumab-RhodG, i.p. | Number of nodules detected, TP, FP, TN, FN |

**Table 2**
Summary of results for animal studies studying HER2-targeted FGCS.

| Author, year | Total resections | TP (%) | FP (%) | TN (%) | FN (%) | Residual disease | Sensitivity | Tumor-to-reference ratio, mean ± SD |
|---|---|---|---|---|---|---|---|---|
| Lee [27] | | | | | | | | 22.2 ± 11.5 [b] |
| Debie [25][a] | NR | | NR (19.6) | | | 2.9% (1.8) | 59.3% | 14.4 ± 8.5 [c] |
| | 249 | | 64 (25.7) | | | 0.7% (0.5) | 95.4% | |
| | 312 | | 19 (6.1) | | | 1.1% (0.6) | 99.0% | |
| Terwisscha [30] | | | | | | | | |
| Kosaka [31] | 69 | 66 (95.7) | | | 3 (4.3) | | | |
| Longmire [32] | 44 | 23 (52.3) | 1 (2.3) | 19 (43.2) | 1 (2.3) | | | |

NR = Not reported.
[a] Upper row represents results of CCS. Middle row represents results of CCS with subsequent FGCS. Lower row represents results of FGCS only.
[b] Tumor-to-muscle ratio.
[c] Tumor-to-background ratio.

## 5. Results

All studies succeeded in fluorescence-guided detection of tumor deposits [26,28,33]. Fluorescent tumor lesions were detected on both the peritoneal wall and intra-abdominal organs [26,28,33]. Tanyi et al. (2017) reported detection of an additional 1–5 tumor nodules per mouse (mean 3.8) with intraoperative fluorescence imaging following CCS [26]. Smallest nodules detected were 5 mm in diameter after visual inspection and palpation and 2 mm in diameter after fluorescence imaging [26]. The average fluorescent signal of tumor deposits was 3.5 times higher than that of adjacent healthy tissue ($p < 0.001$) as reported by Liu et al. (2013) [33]. The TBR of true positive tumor lesions ranged from 0.6–48.2 as reported by Tanyi et al. (2017), with a nonsignificant association suggesting stronger fluorescence in larger nodules [26].

### 5.1. FRα – Human studies

#### 5.1.1. Population and study characteristics

Population and study characteristics are summarized in Table 4. All included studies were non-comparative. Although one study applied a dose-escalation in their methods, results were not separated for the different doses [29]. A total of 74 participants were included, all with known or suspected EOC and scheduled for a surgical staging procedure or cytoreductive surgery. The majority of the participants was diagnosed with advanced stage EOC. The most commonly used imaging system was the Artemis Spectrum. Imaging agents were either OTL38, a folic acid conjugated to a S0456 near-infrared (NIR) dye, or EC17, a folate-FITC conjugate, administered in differing doses.

## 6. Results

Findings are summarized in Table 5. Intraoperative fluorescence imaging was successful for all studies. Patients in the study by Hoogstins et al. (2019) presented without peritoneal metastases, limiting the added value of FGCS. In these patients, only the primary tumor and nine lymph nodes showed fluorescence. All nine resected fluorescent lymph nodes appeared to be false positive after histopathological verification [34]. In a previous study by Hoogstins et al. (2016), of 13 resected fluorescent lymph nodes 11 were false positive [29]. Histopathological verification in both studies found moderate to mild expression of FRβ by macrophages present in the lymph nodes, which is also a binding target of OTL38. Remaining false positive lesions were FRα-expressing uterine and fallopian tissues. Similarly, Randall et al. (2019) reported lymph nodes to be the most common location of false positive resections [35].

Reported true positive values ranged between 75% and 77%, false positive values between 10% and 25% [29,35,36]. False negative and true negative lesions were reported by Randall et al. (2019) only, where 13% of resections appeared to contain tumor but did not fluoresce (false negative) and 1% did not contain tumor and did not fluoresce (true negative) [35]. Sensitivity for detection of FRα-positive tumor lesions was 85.9% (lower 95% CI boundary 81.2%), and positive predictive value (PPV) was 88.1% (lower 95% CI boundary 83.6%) [35].

TBR for true positives was reported by 4 studies, mean ranging from 3.1 to 7.0 [26,29,36,37]. TBR for false positives was reported by 3 studies, mean ranging from 4.4 to 5.4 [29,34,36]. Tummers et al. (2016) and Hoogstins et al. (2016) both reported a statistical insignificant difference between the TBR of true positive and false positive lesions [29,36].

Van Dam et al. (2011) reported a mean duration of in vivo imaging of 10 min (range 4–36 min) [37]. Randall et al. (2019) performed pre-resection imaging for 2 to 23 min. After initial resection the peritoneal cavity was illuminated again to detect residual disease. A second resection had a maximal duration of intraoperative imaging of 46 min [35].

### 6.1. Assessment of video stills

Three studies assessed intra-observer variability of visual detection of tumor deposits by surgeons using video stills in color and fluorescence from intraoperative fluorescence imaging recordings [29,36,37]. Color images were assessed for tumor deposits, after which the

**Table 3**
Population characteristics for animal studies studying FRα-targeted FGCS. Abbreviations: i.p. (intraperitoneally), i.v. (intravenously), TBR (tumor-to-background ratio).

| Author, year | Sex | Age | Type | N | Tumor model | Imaging system | Imaging agent | Outcome |
|---|---|---|---|---|---|---|---|---|
| Liu [33] | | | NSG mice | | Isolated primary cells from patient tumor samples, i.p. | | 2.25 mg/kg PPF, i.v. | TBR, smallest nodule size |
| Hekman [28] | | 6–8 weeks | BALB/c nude mice | 5 | $5 \times 10^6$ IGROV1, i.p. | IVIS Lumina | 10 μg dual-labeled farletuzumab (IRDye800CW, 111In), i.v. | Smallest nodule size |
| Tanyi [26] | Female | 6 weeks | NSG mice | 20 | IGROV1, i.p. | FloCam (Biovision) or prototype system developed by authors | 0.1 mg/kg EC17, i.v. | TBR, smallest nodule size, number of nodules detected |

**Table 4**
Population characteristics of human studies studying FRα-targeted FGCS.

| Author, year | Study design | Ovarian cancer status | Age [a] | N | Imaging agent | Imaging system | Surgery type | Outcome |
|---|---|---|---|---|---|---|---|---|
| Hoogstins [34] | Non-comparative pilot study | Early stage epithelial ovarian cancer FIGO stage Ia-IIIa | 58 ± 8.2 | 6 | 0.0125 mg/kg OTL38 | Artemis Spectrum (Quest) | Laparotomy (3) Laparoscopy (3) | Adverse events, FN, pharmacokinetics, TBR |
| Randall [35] | Single arm, open label, prospective phase II study | Known/suspected epithelial ovarian cancer FIGO stage Ic-IVa | 63.8 ± 0.19 | 44 [b] 29 [c] | 0.025 mg/kg OTL38 | Artemis Spectrum (Quest), PINPOINT (Novadaq), or Visionsense VS3 | n.a. | Imaging duration, adverse events, number of resections, TP, FN, FP, TN, sensitivity, PPV |
| Tanyi [26] | Non-comparative pilot study | Recurrent epithelial ovarian cancer FIGO IIc-IV | 58.8 ± n.a. Range 38–70 | 5 | 0.1 mg/kg EC17 | FloCam (BioVision) or prototype system developed by authors | n.a. | Adverse events, TBR |
| Hoogstins [29] | Dose escalating pilot study | Known/suspected epithelial ovarian cancer FIGO III-IV | Range 49–77 | 12 | 0.0125 mg/kg, 0.025 mg/kg or 0.05 mg/kg OTL38 | Artemis Spectrum (Quest) | Interval debulking (7) Debulking recurrent disease (3) Primary debulking (2) | Assessment of video stills, adverse events, pharmacokinetics, number of resections, TP, FN, FP, TBR |
| Tummers [36] | Non-comparative pilot study | Suspected epithelial ovarian cancer FIGO IIb-IV | 62.5 ± 10.8 | 12 | 0.1 mg/kg EC17 | Artemis Spectrum (Quest) | Primary cytoreductive procedure (6) Interval cytoreductive procedure (4) Staging procedure (2) | Assessment of video stills, adverse events, pharmacokinetics, number of resections, TP, FN, FP, TBR |
| Van Dam [37] | Non-comparative pilot study | Suspected epithelial ovarian cancer FIGO I-III | 61.2 ± 11.4 | 10 | 0.3 mg/kg EC17 | EM-CCD fluorescence camera with PCO-AG color camera | n.a. | Imaging duration, smallest tumor nodule, assessment of video stills, adverse events, TBR |

Abbreviations: n.a. (not available), PPV (positive predictive value).
[a] Mean ± SD, when not available range is given.
[b] N patients included in safety analysis.
[c] N patients included in efficacy analysis.

**Table 5**
Summary of results for human studies studying FRα-targeted FGCS. Abbreviations: l.b. (lower boundary), 95% CI (95% confidence interval).

| Author, year | Half-life, minutes | Resections | TP (%) | FP (%) | TN (%) | FN (%) | Sensitivity (l.b. 95% CI) | PPV (l.b. 95% CI) | TBR TP, mean ± SD | TBR FP, mean ± SD | Nodules detected, color still | Nodules detected, fluorescent still |
|---|---|---|---|---|---|---|---|---|---|---|---|---|
| Van Dam [37] | | | | | | | | | 3.1 ± 0.8 | | Median 7, range 4–22 | Median 34, range 8–81 |
| Tummers [36] | 86.8 | 57 | 44 (77) | 13 (23) | | | | | 7.0 ± 1.2 | 5.4 ± 1.0 | Mean 23.3, SD 11.9 | Mean 39.6, SD 22.7 |
| Hoogstins [29] | 120–180 | 83 | 62 (75) | 21 (25) | | | | | 4.4 ± 1.46 | 5.4 ± 2.0 | Mean 8.3, SD 5.4 | Mean 17.6, SD 10.8 |
| Randall [35] | | 225 | 171 (76) | 23 (10) | 3 (1) | 28 (13) | 85.9% (81.2) | 88.1% (83.6) | | | | |
| Tanyi [27] | | | | 0 | | | | | 6.3 ± 4.9 | | | |
| Hoogstins [34] | 120–180 | | | 9 | | 0 | | | | 4.4 ± 3.3 | | |

matching fluorescence images were assessed. Mean number of detected tumor deposits increased 1.7–2.1 times and median increased from 7 to 34 in favor of fluorescence images compared to color images.

### 6.2. Practical evaluation

Using a 5-question questionnaire, the practical evaluation of FGCS and intraoperative fluorescence imaging by gynaecological oncologists was explored. Results showed that fluorescence imaging did not interfere with cytoreductive surgery performance. The technique was found to be useful by the majority of participating surgeons [29].

### 6.3. Pharmacokinetics and adverse events

Both studies by Hoogstins et al. (2016, 2019) reported a half-life of 120–180 min for OTL38 [29,34]. Tummers et al. (2016) reported a half-life of 86.8 min for EC17 [36]. All studies reported on adverse events [26,29,34–37]. Adverse events occurred in 18–47% of participants. Most common adverse events related to the imaging agent were abdominal discomfort, abdominal pain, nausea and hypersensitivity symptoms such as itching throat, pruritus and sneezing. Frequency of adverse events increased with dose in a single dose-escalating study [29].

## 7. Discussion

We aimed to review the scientific literature on the feasibility of FGCS targeting HER2- or FRα-expressing EOC. All animal studies showed clear feasibility of intraoperative fluorescence-guided detection of EOC tumor deposits. In addition, one HER2-targeted study reported promising test statistics suggesting superiority of FGCS over CCS in the detection of tumor lesions. Subsequent human studies on FRα confirmed feasibility with similar results for test statistics and TBR. The severity of adverse events was limited.

Feasibility of the intervention is determined by multiple factors besides test statistics. Patients receive the imaging agent via intravenous infusion 2-4 h before surgery and medical supervision is needed due to the possibility of adverse events and subsequent treatment. The use of fluorescence imaging extended the length of surgery in the included studies. However, in clinical practice surgical time might be reduced due to efficient localization of tumor deposits with intraoperative fluorescence imaging. Intraoperative fluorescence imaging devices vary in costs, depending on the complexity and quality of the device [38]. No long-term toxicity or any postoperative complications related to the imaging agents were reported.

Although intra-peritoneally spread metastases were located with a detection accuracy of 75–77% (true positive) in pilot studies, false positives were substantial, ranging from 10% to 25%. Most of the false positive lesions were lymph nodes harboring macrophages expressing FRβ, another target for OTL38 and EC17 [29,34–36]. This suggests that lymph node metastases cannot be accurately detected with these imaging agents. Currently, resection of enlarged lymph nodes is included in the surgical treatment of advanced EOC. Enlarged lymph nodes can be detected by preoperative CT-scan and intraoperative palpation. Though lymph nodes detected with a preoperative CT-scan are sometimes difficult to locate during surgery and the sensitivity of lymph node palpation is limited [39–41]. Targeted FGCS could still be of use to accurately detect metastatic lymph nodes and reduce postoperative complications caused by unwarranted lymph node resection [42]. To accomplish this, the targeting component can be changed to one less likely to cross-react with other targets or different imaging agents with multiple targets can be combined. For example, metastatic lymph nodes could be detected with fluorescence imaging in animal models of head and neck cancer using the αvβ3 integrin as a target [43]. This integrin is also overexpressed in some EOCs and shows promising results as a target in FGCS on EOC animal-models [44–46]. An additional reason to include multiple imaging agents, and thereby targeting different EOC markers, is

intra-tumor heterogeneity. Subclonal EOC populations demonstrate variable treatment sensitivity and are able to expand during chemotherapy [47,48]. Increasing the number of imaging agents and targets could overcome the limitations of subclonality.

Intraoperative fluorescence imaging is affected by scattering, absorption and autofluorescence [49]. In the NIR range, tissue penetration can be >1 cm due to lower tissue absorption. In comparison, visible light is highly absorbed by tissue, limiting penetration depth to a few millimeters (at 400 nm emission) to a maximum of 1 cm (at 700 nm emission). Autofluorescence, caused by excitation of endogenous fluorophores, is much lower in the NIR range compared to visible light. The effect of scattering can be beneficial or detrimental for the fluorescence signal intensity and accuracy of signal detection, depending on the tissue characteristics. Of the imaging agents included, the fluorophores PPF, IRDye800CW, AlexaFluor680 and imaging agent OTL38 are in the NIR spectrum. Imaging agent EC17 and fluorophore Rhodamine Green emit in green in the visible spectrum. In a study comparing fluorescent properties of OTL38 and EC17 in animal models, signal-to-background ratio (SBR) was 3.3-fold higher for OTL38 and autofluorescence was minimal compared to EC17 [50]. This suggests OTL38 is superior to EC17 regarding fluorescence characteristics and most suitable for future experiments.

Since FRα is more often overexpressed in EOC compared to HER2 and a fluorophore emitting in the NIR region is more suitable compared to one emitting in the visible spectrum, future studies focusing on targeting FRα with an NIR-fluorophore conjugate seem to be most promising. Although FRα is overexpressed in 80% of the EOC cases, the expression levels for different subtypes of EOC is difficult to accurately report in literature because most subtypes are rare [9,51,52]. In clinical practice, the histological subtype would not matter for FGCS eligibility. Every patient diagnosed with EOC would be screened for FRα status and if positive, FRα-targeted FGCS would be an additional treatment option. The feasibility of FRα-targeted FGCS has been demonstrated by both animal and human studies. The goal of this intervention is to identify occult disease and residual disease during surgical staging or cytoreductive surgery in patients diagnosed with EOC of all stages and may consequently increase survival, although these outcomes have not been studied yet. A randomized controlled trial (RCT) is needed in patients with advanced stage EOC positive for FRα to assess survival benefits. To assess sensitivity and specificity, CCS should be compared with CCS supplemented by FGCS in two randomized groups of patients with EOC. Histological confirmation of all resected lesions should act as the reference standard. Follow-up should be long enough to report on recurrence rates and survival outcome. Secondary endpoints should at least include adverse events, additional costs and surgery duration. To further optimize FGCS, high magnification fluorescence cameras should be implemented to aid detection of fluorescent tumor lesions invisible to the naked eye.

One of the limitations of this review was the risk of bias assessment of human studies. Since all studies applied a non-comparative design, there was no fitting risk of bias tool to assess these studies. A second limitation is the variability in imaging agents and doses and inclusion of both human and animal studies (i.e. methodological heterogeneity), which prevented pooling of the results via a meta-analysis. However, including both human and animal studies on a narrow subject gives a broader perspective of available results. Finally, risk of bias assessment was mostly unclear or negative for animal studies. This is not exceptional, since animal study designs are often flawed or reported incompletely and results are hard to reproduce [53–55]. Still, systematic reviews of animal studies are valuable for data translation to clinical practice [56].

## 8. Conclusion

FGCS is a promising technique that has the potential to improve surgical cytoreduction with a decrease in residual disease. Results for HER2-targeted FGCS suggest feasibility, but further research is needed to confirm current results and to advance to a pilot study including patients with HER2-positive EOC. FRα-targeted FGCS demonstrated to be feasible and diagnostically valuable in both EOC animal models and patients with EOC. A randomized controlled trial is needed to validate preliminary results and quantify its effect on progression free and overall survival.

## Author statement

JJ and CG were involved in the conceptualization. JJ obtained and interpreted data, with support from CG and JH. JJ wrote the first draft of the manuscript. JJ and CG critically revised the manuscript. All authors were involved in writing the manuscript and approved the final version.

## Declaration of Competing Interest

The authors declare that they have no conflicts of interest.

## Appendix A. Supplementary data

Supplementary data to this article can be found online at https://doi.org/10.1016/j.ygyno.2021.05.017.

## References

[1] R. Bretveld, O. van der Hel, M. van der Aa, S. Verboort, Ovarium carcinoom in Nederland, 2019.
[2] Y. Dabi, et al., Patients with stage IV epithelial ovarian cancer: understanding the determinants of survival, J. Transl. Med. 18 (2020) 134.
[3] R.E. Bristow, R.S. Tomacruz, D.K. Armstrong, E.L. Trimble, F.J. Montz, Survival effect of maximal cytoreductive surgery for advanced ovarian carcinoma during the platinum era: a meta-analysis, J. Clin. Oncol. Off. J. Am. Soc. Clin. Oncol. 20 (2002) 1248–1259.
[4] S.-J. Chang, R.E. Bristow, H.-S. Ryu, Impact of complete cytoreduction leaving no gross residual disease associated with radical cytoreductive surgical procedures on survival in advanced ovarian cancer, Ann. Surg. Oncol. 19 (2012) 4059–4067.
[5] S. Wallace, et al., Efforts at maximal cytoreduction improve survival in ovarian cancer patients, even when complete gross resection is not feasible, Gynecol. Oncol. 145 (2017) 21–26.
[6] A. du Bois, et al., Role of surgical outcome as prognostic factor in advanced epithelial ovarian cancer: a combined exploratory analysis of 3 prospectively randomized phase 3 multicenter trials: by the Arbeitsgemeinschaft Gynaekologische Onkologie Studiengruppe Ovarialkarzi, Cancer 115 (2009) 1234–1244.
[7] S. Hernot, L. van Manen, P. Debie, J.S.D. Mieog, A.L. Vahrmeijer, Latest developments in molecular tracers for fluorescence image-guided cancer surgery, Lancet Oncol. 20 (2019) e354–e367.
[8] N. Parker, et al., Folate receptor expression in carcinomas and normal tissues determined by a quantitative radioligand binding assay, Anal. Biochem. 338 (2005) 284–293.
[9] K.R. Kalli, et al., Folate receptor alpha as a tumor target in epithelial ovarian cancer, Gynecol. Oncol. 108 (2008) 619–626.
[10] S. Markert, et al., Alpha-folate receptor expression in epithelial ovarian carcinoma and non-neoplastic ovarian tissue, Anticancer Res. 28 (2008) 3567–3572.
[11] J.D. Predina, et al., Localization of pulmonary ground-glass opacities with folate receptor-targeted intraoperative molecular imaging, J. Thorac. Oncol. Off. Publ. Int. Assoc. Study Lung Cancer 13 (2018) 1028–1036.
[12] J.D. Predina, et al., Identification of a folate receptor-targeted near-infrared molecular contrast agent to localize pulmonary adenocarcinomas, Mol. Ther. 26 (2018) 390–403.
[13] J.D. Predina, et al., Intraoperative molecular imaging combined with positron emission tomography improves surgical Management of Peripheral Malignant Pulmonary Nodules, Ann. Surg. 266 (2017) 479–488.
[14] Y.W. Chung, et al., Overexpression of HER2/HER3 and clinical feature of ovarian cancer, J. Gynecol. Oncol. 30 (2019), e75.
[15] E. Lanitis, et al., Primary human ovarian epithelial cancer cells broadly express HER2 at immunologically-detectable levels, PLoS One 7 (2012), e49829.
[16] E. Verri, et al., HER2/neu oncoprotein overexpression in epithelial ovarian cancer: evaluation of its prevalence and prognostic significance. Clinical study, Oncology 68 (2005) 154–161.
[17] Y. Yarden, M.X. Sliwkowski, Untangling the ErbB signalling network, Nat. Rev. Mol. Cell Biol. 2 (2001) 127–137.
[18] D.-Y. Oh, Y.-J. Bang, HER2-targeted therapies - a role beyond breast cancer, Nat. Rev. Clin. Oncol. 17 (2020) 33–48.
[19] Meric-Bernstam, F. *et al.* Advances in HER2-targeted therapy: novel agents and opportunities beyond breast and gastric cancer. Clin. cancer Res. an Off. J. Am. Assoc. Cancer Res. 25, 2033–2041 (2019).

[20] S.B. Lee, et al., Affibody molecules for in vivo characterization of HER2-positive tumors by near-infrared imaging, Clin. cancer Res. an Off. J. Am. Assoc. Cancer Res. 14 (2008) 3840–3849.
[21] Y. Koyama, et al., Spectral fluorescence molecular imaging of lung metastases targeting HER2/neu, Clin. cancer Res. an Off. J. Am. Assoc. Cancer Res. 13 (2007) 2936–2945.
[22] K. Slim, et al., Methodological index for non-randomized studies (minors): development and validation of a new instrument, ANZ J. Surg. 73 (2003) 712–716.
[23] C.R. Hooijmans, et al., SYRCLE's risk of bias tool for animal studies, BMC Med. Res. Methodol. 14 (2014) 43.
[24] J.P.T. Higgins, et al., The Cochrane Collaboration's tool for assessing risk of bias in randomised trials, BMJ 343 (2011) d5928.
[25] P. Debie, et al., Improved Debulking of peritoneal tumor implants by near-infrared fluorescent Nanobody image guidance in an experimental mouse model, Mol. Imaging Biol. 20 (2018) 361–367.
[26] J.L. Tanyi, et al., Intraoperative molecular imaging can identify sub-centimeter peritoneal implants during ovarian cancer cytoreductive surgery, Eur. J. Gynaecol. Oncol. 38 (2017) 589–595.
[27] H.J. Lee, et al., Dual-labeled pertuzumab for multimodality image-guided ovarian tumor resection, Am. J. Cancer Res. 9 (2019) 1454–1468.
[28] M.C.H. Hekman, et al., Improved intraoperative detection of ovarian Cancer by folate receptor alpha targeted dual-modality imaging, Mol. Pharm. 14 (2017) 3457–3463.
[29] C.E.S. Hoogstins, et al., A novel tumor-specific agent for intraoperative near-infrared fluorescence imaging: a translational study in healthy volunteers and patients with ovarian cancer, Clin. Cancer Res. 22 (2016) 2929–2938.
[30] A.G.T.T. van Scheltinga, et al., Intraoperative near-infrared fluorescence tumor imaging with vascular endothelial growth factor and human epidermal growth factor receptor 2 targeting antibodies, J. Nucl. Med. 52 (2011) 1778–1785.
[31] N. Kosaka, M. Ogawa, M.R. Longmire, P.L. Choyke, H. Kobayashi, Multi-targeted multi-color in vivo optical imaging in a model of disseminated peritoneal ovarian cancer, J. Biomed. Opt. 14 (2009) 14023.
[32] M. Longmire, et al., Multicolor in vivo targeted imaging to guide real-time surgery of HER2-positive micrometastases in a two-tumor coincident model of ovarian cancer, Cancer Sci. 100 (2009) 1099–1104.
[33] T.W. Liu, et al., Biologically-targeted detection of primary and micro-metastatic ovarian cancer, Theranostics 3 (2013) 420–427.
[34] C.E.S. Hoogstins, et al., Feasibility of folate receptor-targeted intraoperative fluorescence imaging during staging procedures for early ovarian cancer, Eur. J. Gynaecol. Oncol. 40 (2019) 203–208.
[35] L.M. Randall, R.M. Wenham, P.S. Low, S.C. Dowdy, J.L. Tanyi, A phase II, multicenter, open-label trial of OTL38 injection for the intra-operative imaging of folate receptor-alpha positive ovarian cancer, Gynecol. Oncol. 155 (2019) 63–68.
[36] Q.R.J.G. Tummers, et al., Intraoperative imaging of folate receptor alpha positive ovarian and breast cancer using the tumor specific agent EC17, Oncotarget 7 (2016) 32144–32155.
[37] G.M. van Dam, et al., Intraoperative tumor-specific fluorescence imaging in ovarian cancer by folate receptor-alpha targeting: first in-human results, Nat. Med. 17 (2011) 1315–1319.
[38] A.V. DSouza, H. Lin, E.R. Henderson, K.S. Samkoe, B.W. Pogue, Review of fluorescence guided surgery systems: identification of key performance capabilities beyond indocyanine green imaging, J. Biomed. Opt. 21 (2016) 80901.
[39] H.A. Arango, et al., Accuracy of lymph node palpation to determine need for lymphadenectomy in gynecologic malignancies, Obstet. Gynecol. 95 (2000) 553–556.
[40] G.H. Eltabbakh, Intraoperative clinical evaluation of lymph nodes in women with gynecologic cancer, Am. J. Obstet. Gynecol. 184 (2001) 1177–1181.
[41] S. Tangjitgamol, S. Manusirivithaya, S. Jesadapatarakul, S. Leelahakorn, T. Thawaramara, Lymph node size in uterine cancer: a revisit, Int. J. Gynecol. cancer Off. J. Int. Gynecol. Cancer Soc. 16 (2006) 1880–1884.
[42] P. Harter, et al., A randomized trial of lymphadenectomy in patients with advanced ovarian neoplasms, N. Engl. J. Med. 380 (2019) 822–832.
[43] I. Atallah, et al., Role of near-infrared fluorescence imaging in the resection of metastatic lymph nodes in an optimized orthotopic animal model of HNSCC, Eur. Ann. Otorhinolaryngol. Head Neck Dis. 132 (2015) 337–342.
[44] E. Mery, et al., Intraoperative fluorescence imaging of peritoneal dissemination of ovarian carcinomas. A preclinical study, Gynecol. Oncol. 122 (2011) 155–162.
[45] N.J. Harlaar, et al., Real-time near infrared fluorescence (NIRF) intra-operative imaging in ovarian cancer using an alpha(v)beta(3-)integrin targeted agent, Gynecol. Oncol. 128 (2013) 590–595.
[46] E. Mery, et al., Fluorescence-guided surgery for cancer patients: a proof of concept study on human xenografts in mice and spontaneous tumors in pets, Oncotarget 8 (2017) 109559–109574.
[47] R.F. Schwarz, et al., Spatial and temporal heterogeneity in high-grade serous ovarian cancer: a phylogenetic analysis, PLoS Med. 12 (2015), e1001789.
[48] A. Bashashati, et al., Distinct evolutionary trajectories of primary high-grade serous ovarian cancers revealed through spatial mutational profiling, J. Pathol. 231 (2013) 21–34.
[49] S. Keereweer, et al., Optical image-guided cancer surgery: challenges and limitations, Clin. cancer Res. an Off. J. Am. Assoc. Cancer Res. 19 (2013) 3745–3754.
[50] E. De Jesus, et al., Comparison of Folate Receptor Targeted Optical Contrast Agents for Intraoperative Molecular Imaging, Int. J. Mol. Imaging 2015 (2015) 469047.
[51] L.M.A. Crane, et al., The effect of chemotherapy on expression of folate receptor-alpha in ovarian cancer, Cell. Oncol. (Dordr). 35 (9–18) (2012).
[52] S. Senol, et al., Folate receptor α expression and significance in endometrioid endometrium carcinoma and endometrial hyperplasia, Int. J. Clin. Exp. Pathol. 8 (2015) 5633–5641.
[53] C. Kilkenny, et al., Survey of the quality of experimental design, statistical analysis and reporting of research using animals, PLoS One 4 (2009), e7824.
[54] F. Prinz, T. Schlange, K. Asadullah, Believe it or not: how much can we rely on published data on potential drug targets? Nat. Rev. Drug Discov. 10 (2011) 712.
[55] M.T. Avey, et al., The devil is in the details: incomplete reporting in preclinical animal research, PLoS One 11 (2016), e0166733.
[56] J. van Luijk, et al., Systematic reviews of animal studies; missing link in translational research? PLoS One 9 (2014), e89981.